Measurement Science and Technology

"This is an author-created, un-copyedited version of an article accepted for publication/published in Measurement Science and Technology. IOP Publishing Ltd is not responsible for any errors or omissions in this version of the manuscript or any version derived from it. The Version of Record is available online at DOI: 10.1088/1361-6501/ac2ca5

ACCEPTED MANUSCRIPT

Simultaneous measurements of velocity, gas concentration, and temperature by way of thermal-anemometry-based probes

To cite this article before publication: Alaïs Hewes et al 2021 Meas. Sci. Technol. in press https://doi.org/10.1088/1361-6501/ac2ca5

Manuscript version: Accepted Manuscript

Accepted Manuscript is "the version of the article accepted for publication including all changes made as a result of the peer review process, and which may also include the addition to the article by IOP Publishing of a header, an article ID, a cover sheet and/or an 'Accepted Manuscript' watermark, but excluding any other editing, typesetting or other changes made by IOP Publishing and/or its licensors"

This Accepted Manuscript is © 2021 IOP Publishing Ltd.

During the embargo period (the 12 month period from the publication of the Version of Record of this article), the Accepted Manuscript is fully protected by copyright and cannot be reused or reposted elsewhere.

As the Version of Record of this article is going to be / has been published on a subscription basis, this Accepted Manuscript is available for reuse under a CC BY-NC-ND 3.0 licence after the 12 month embargo period.

After the embargo period, everyone is permitted to use copy and redistribute this article for non-commercial purposes only, provided that they adhere to all the terms of the licence https://creativecommons.org/licences/by-nc-nd/3.0

Although reasonable endeavours have been taken to obtain all necessary permissions from third parties to include their copyrighted content within this article, their full citation and copyright line may not be present in this Accepted Manuscript version. Before using any content from this article, please refer to the Version of Record on IOPscience once published for full citation and copyright details, as permissions will likely be required. All third party content is fully copyright protected, unless specifically stated otherwise in the figure caption in the Version of Record.

View the article online for updates and enhancements.

Simultaneous measurements of velocity, gas concentration, and temperature by way of thermal-anemometry-based probes

Alaïs Hewes and Laurent Mydlarski

Department of Mechanical Engineering, McGill University, 817 Sherbrooke St. W., Montreal, QC H3A 0C3, Canada

E-mail: laurent.mydlarski@mcgill.ca

April 2021

Abstract.

Many natural and engineering flows transport more than one scalar. Moreover, to study the scalar mixing therein, knowledge of the velocity field is also essential. For this reason, the present work describes the development of a three-wire thermalanemometry-based probe to simultaneously measure velocity, helium concentration, and temperature in turbulent flows. It is first demonstrated, both theoretically and experimentally, that the temperature measured by a cold-wire thermometer is effectively insensitive to helium concentration. Then, building on recent work by Hewes and Mydlarski (Meas. Sci. Technol., 2021), which pertains to the design of interference probes (i.e. thermal-anemometry-based probes used to measure velocity and gas concentration), a novel temperature compensation technique is proposed to extend their use to non-isothermal flows. The performance of the compensation technique is validated in turbulent coaxial jets by combining the cold-wire thermometer and interference probe to form the three-wire probe. Given that the three-wire probe can be employed to obtain simultaneous measurements of velocity and multiple scalars, it can therefore be used investigate phenomena such as multi-scalar mixing, including differential diffusion.

Submitted to: Meas. Sci. Technol.

1. Introduction

Many natural and engineering flows transport more than one scalar (i.e. temperature, humidity, concentration of a chemical species). A complete description of the turbulent multi-scalar mixing process that can occur in such flows (e.g. the mixing of temperature and salinity in the ocean, mixing of temperature and humidity in the atmosphere, or the mixing of reactants and products in combusting flows) requires that simultaneous multi-scalar and velocity measurements be performed with high spatial and temporal resolutions. However, such measurements are complex, and, to the author's knowledge, have only been performed once before [1].

Thermal anemometry is well suited to making simultaneous multi-scalar and velocity measurements, largely due to its versatility. Although thermal-anemometry is commonly used to measure velocity in turbulent flows [2–5], it can also be adapated to measure temperature (e.g. cold-wire thermometers [6–8]) or concentration in a gas mixture (e.g. thermal-anemometry-based aspirating probes, [9–15]). Moreover, simultaneous velocity-scalar measurements can be performed by combining different thermal-anemometry-based sensors. For example, hot-wire anemometers and cold-wire thermometers can be used together to simultaneously measure velocity and temperature [16–22]. Similarly, two hot-wires and/or hot-films with different characteristics, or ones placed close enough together that their thermal fields interfere, can be used to simultaneously measure velocity and gas concentration [23–32]. The latter may be referred to as interference probes and are described in greater detail in Hewes and Mydlarski [32], as well as in §4.1 of the present work.

To simultaneously measure multiple scalars and velocity, Sirivat and Warhaft [1] combined (i) an interference probe with (ii) a single-normal hot-wire sensor operated at a low overheat ratio. The former was used to measure velocity and helium concentration independently of temperature, and the latter was used to infer the temperature of the flow. Although Sirivat and Warhaft [1] successfully used this combined 3-wire probe to study the mixing of both temperature and helium in grid-generated turbulence, it had one significant limitation; the probe was primarily designed for flows with small temperature fluctuations ($\theta_{rms} < 0.1$ °C), such that their interference probe – which consisted of two hot-wires spaced closely together – could be assumed to be insensitive to the surrounding temperature of the flow. As will be shown in §4.2, this assumption is not necessarily valid in other non-isothermal flows.

Subsequent experimental studies of multi-scalar mixing focused only on the scalar fields of the flow and did not measure the velocity field of the flow [33–41]. Thus, there do not appear to have been any additional attempts to develop other multi-scalar and velocity measurement techniques since the work of Sirivat and Warhaft [1], much less those which could be used in a wider range of flows. To rectify this situation, and make simultaneous two-scalar and velocity measurements in a larger class of flows, we therefore develop a novel 3-wire thermal-anemometry-based probe. In contrast to the probe designed by Sirivat and Warhaft, our 3-wire probe consists of a cold-wire

 Simultaneous measurements of U, C, and T

thermometer (which is used to measure temperature independently of velocity and helium concentration) and an interference probe (which is used to infer velocity and helium concentration). To use the interference probe, and by extension the 3-wire probe, in non-isothermal flows with large temperature fluctuations ($\theta_{rms} \gg 0.1$ °C), we formulate a novel temperature compensation technique for the interference probe.

The remainder of this paper describes the development of the novel 3-wire probe, specifically focusing on the temperature compensation method. It is organized as follows. The experimental apparatus used to calibrate and test the novel 3-wire probe is described in §2. In §3, we demonstrate that the temperature measured by a cold-wire thermometer is effectively insensitive to the fluid's helium concentration (just as it has previously been shown to be effectively insensitive to the fluid's velocity [4]). Then, §4 and §5 respectively discuss and validate the temperature compensation method for the interference probe. Finally, conclusions are presented in §6.

2. Experimental Apparatus

The experimental apparatus, including the (i) calibration apparatus, (ii) apparatus for validation measurements, and (iii) data acquisition system is described below. Additional details can be found in Hewes [42].

2.1. Calibration Apparatus

Both the interference probe and cold-wire thermometer were calibrated in a commercially produced TSI Model 1128B Air Velocity Calibrator modified to generate laminar, uniform velocity flows of varying helium concentrations and temperatures. He/air mixtures were produced far upstream of the calibration jet by joining a continuous stream of helium with a continuous stream of air, as depicted in figure 1. The flow rate of the air was set with a needle valve and measured with a 100 slpm mass flow meter (Alicat M-100SLPM-D), and the flow rate of the helium was controlled with a 20 slpm mass flow controller (Alicat MC-20SLPM-D). An automated, custom-made LabVIEW program was used to set the helium flow rate and maintain mixtures of constant helium concentrations. The He/air mixtures were then heated in a long copper cylinder to which three 80 Ω strip heaters were attached. The velocity at exit of the calibration jet was inferred from the sum of the measurements of the mass flow meter and mass flow controller, and the temperature was measured with a type-E thermocouple installed at the jet exit.

2.2. Apparatus for Validation Measurements

Validation measurements were performed in a flow consisting of three concentric jets: (i) a center jet containing an (unheated) mixture of helium and air, (ii) an annular jet containing pure (unheated) air, and (iii) a coflow containing (pure) heated air (see figure 2). The center jet and annular jet (with dimensions listed in table 1) are designed to

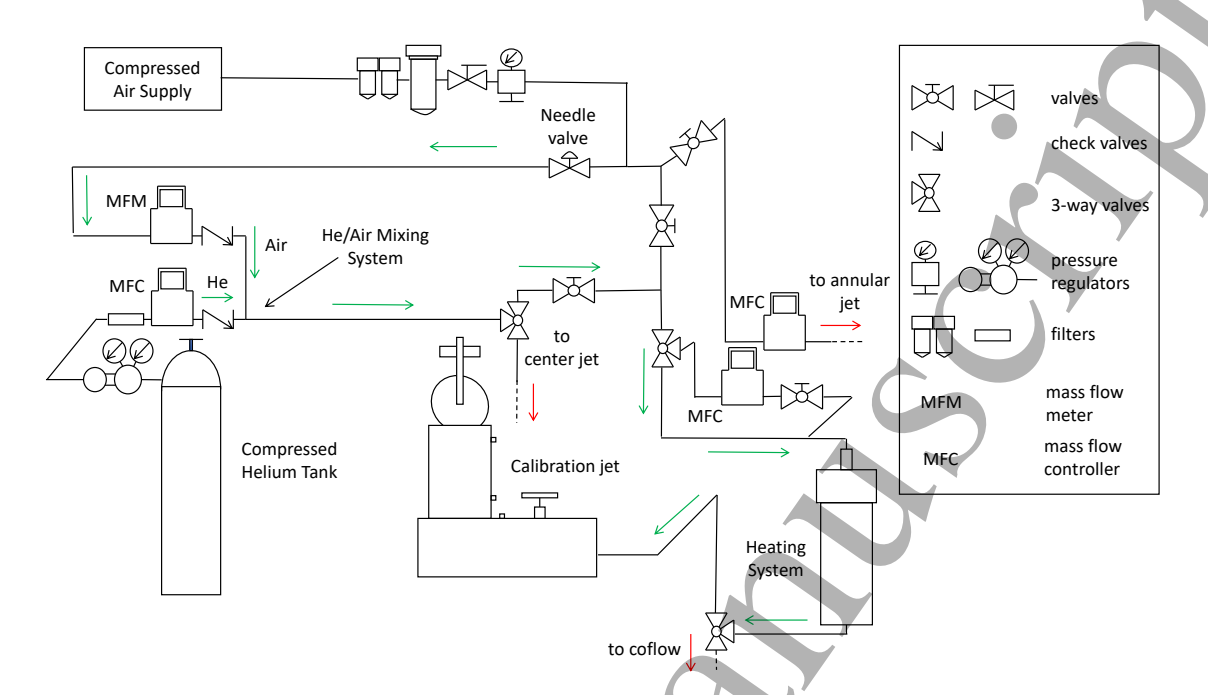


Figure 1: Schematic of the calibration apparatus. Green arrows denote the path of fluid flow during calibrations. Red arrows denote the interface with the coaxial jet apparatus used for validation measurements.

Table 1: Dimensions for the center jet, annular jet, and coflow

Jet	D_i (mm)	$D_o \text{ (mm)}$
Center jet	-	6.22
Annular jet	9.53	12.7
Coflow	19.1	149

have fully-developed velocity profiles at their exits, whereas the coflow (with dimensions also listed in table 1) is designed to generate a uniform velocity profile with minimal velocity fluctuations at its exit. All three jets are connected to the calibration apparatus depicted in figure 1, and the entire coaxial jet apparatus is housed in a large $1.8 \text{ m} \times 1.7 \text{ m} \times 2.4 \text{ m}$ enclosure, which shields it from external flow perturbations. Velmex BiSlide traversing mechanisms mounted next to the coaxial jets were used to support the 3-wire probe, and translate it in three directions [42].

2.3. Data Acquisition

The two wires comprising the interference probe were operated using two channels of a TSI IFA300 Constant Temperature Anemometer (CTA), and the cold-wire thermometer was operated using a custom-made constant current anemometer built at the Université Laval in Québec, Canada [6]. The analog signals from each of these anemometers were digitized using a 16-bit National Instrument PCI-6143 data acquisition board. During

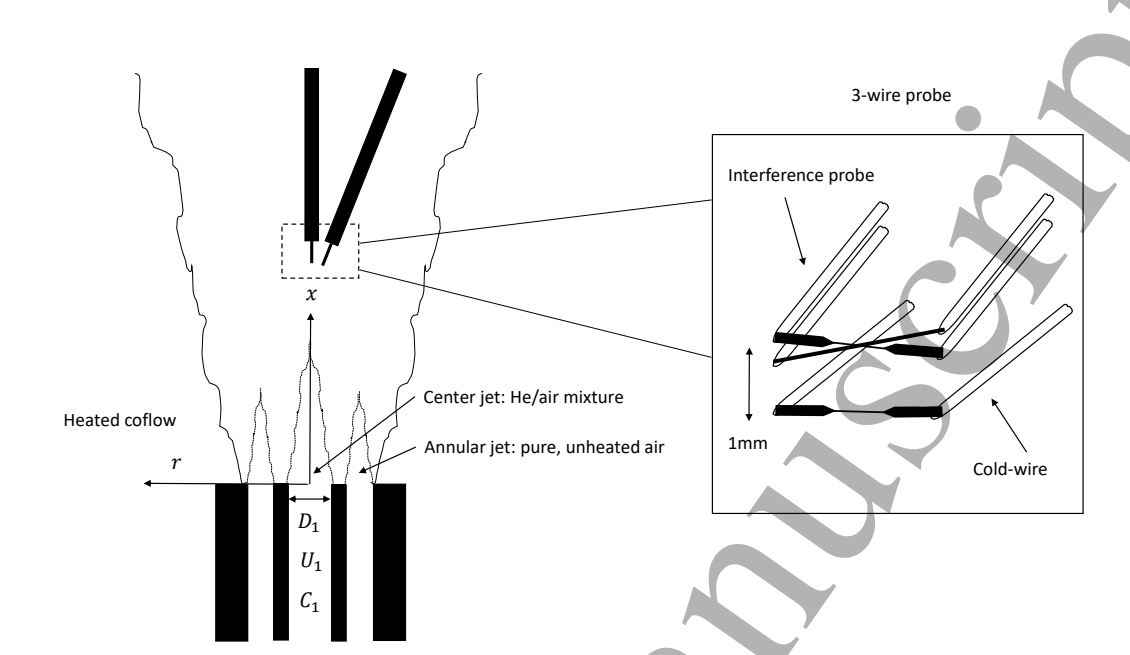


Figure 2: Schematic of the coaxial jet apparatus and 3-wire probe. The center jet, annular jet, and coflow will respectively be denoted using subscripts 1, 2 and 3.

validation measurements, signals from the interference probe and cold-wire were bandpass filtered with Krohn-Hite 3382 and 3384 filters, and amplified, if necessary. Time series of the data were obtained by sampling 3.3×10^7 points at twice the low-pass frequency (10 – 80 kHz, depending on the downstream distance).

3. Insensitivity of Cold-wire Thermometers to Helium Concentration

A cold-wire thermometer is a fine wire $(d \lesssim 1\,\mu\text{m})$, typically of platinum or platinum-rhodium, operated as a resistance temperature detector (RTD) in conjunction with a constant current source. If the current is low $(I \sim 0.1 \text{ mA})$, the cold-wire is nearly insensitive to the fluctuating velocity field of a turbulent flow [4], and only measures the temperature fluctuations of this flow. Although cold-wire thermometers have principally been used in flows of pure air, we will show herein that they can also be used in He/air mixtures (in the range $0 \leq C \leq 0.06$, where C is the mass fraction of helium). We emphasize that this is not evident a priori, given that a cold-wire thermometry sensor is nevertheless heated to a temperature above that of its surrounding, and its measurement of temperature may depend on the ensuing heat transfer, which itself can depend on the fluid properties and/or velocity.

To do so, we analyze the heat transfer relationship for a cold-wire of length l and diameter d through which an electrical current I passes. Assuming that heat transfer by conduction and radiation is negligible, one can derive the following expression relating the voltage measured across the cold-wire (E) to the properties of the fluid flow (see

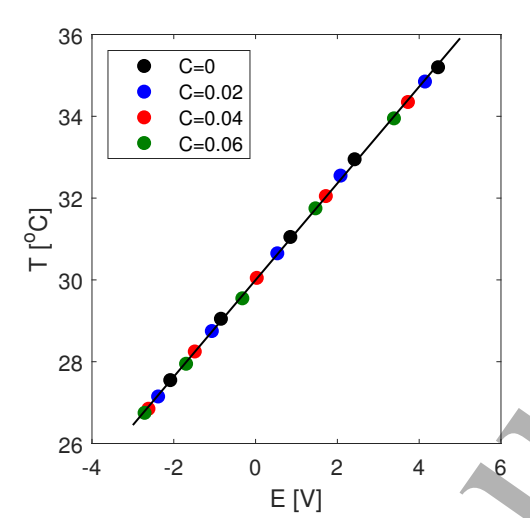


Figure 3: Calibration of a 0.63 μ m diameter platinum cold-wire in flows of different helium concentrations (C) with a linear best-fit line fit to the data. The velocity at which each calibration was performed is constant and equal to 7 m/s, and the voltage measured by the cold-wire is compared to the temperature measured by a type-E thermocouple.

Chapter 7 of Bruun [4]):

$$\tau_w \frac{dE}{dt} + E = I \frac{\pi l k \text{Nu}}{\pi l k \text{Nu} - \alpha_{20} R_{20} I^2} R_a, \tag{1}$$

where
$$\tau_w$$
, defined as follows:
$$\tau_w = \frac{\rho_w c_w(\pi/4) d^2 l}{\pi l k \text{Nu} - \alpha_{20} R_{20} I^2},$$
 (2)

is the time-constant of the wire. Since cold-wires are generally operated with very low currents (hence their name), $\tau_w \approx \rho_w c_w d^2/4k$ Nu, and the above equation can be approximated as follows:

$$\tau_w \frac{dE}{dt} + E \approx IR_a. \tag{3}$$

If τ_w is small (which is usually the case, given that cold-wires have small diameters to have high frequency responses), then

$$E \approx IR_a = IR_{20}[1 + \alpha_{20}(T - T_{20})]. \tag{4}$$

Thus, (if the above assumptions are sufficiently accurate) E does not depend on velocity, and also does not depend on helium concentration.

The independence of E on helium concentration was confirmed experimentally in figure 3, in which a platinum cold-wire similar to that employed in Lepore and Mydlarski [7] ($d = 0.63 \,\mu\text{m}$, $l/d \approx 800$, operated at a current of 0.1 mA) was calibrated in constant-velocity flows of different helium concentrations (U = 7.0 m/s, 0 < C < 0.06). As may be observed in this figure, the calibrations performed at different concentrations

See Appendix A for a complete nomenclature.

all collapse onto a single straight line, such that:

$$E = A + BT, (5$$

where neither A nor B are functions of helium concentration.

This experiment was repeated a total of 10 times with similar results. In each case, the uncertainty of the fitted data (e.g. figure 3), which can be used to characterize the uncertainty resulting from differences in helium concentration, was found to be approximately 0.05° C. Moreover, using a similar analysis, we also assessed the effects of velocity on the cold-wire measurements to ensure that, as predicted, the cold-wire was also insensitive to velocity. We have found that the uncertainty from calibrations performed at different velocities (5-15 m/s) was approximately 0.09° C. The above uncertainties are comparable to those which occur during the calibration of cold-wires in pure air at a single velocity $(0.04-0.14^{\circ}\text{C }[42,43])$, which further suggests that any sensitivity to helium concentration or velocity is negligible. Thus, it can be concluded that a cold-wire can be used to measure temperature in He/air mixtures with similar accuracies and limitations to those in a flow of pure air.

4. Temperature Compensation Method for Interference Probes

The current section describes the temperature compensation method for the interference probe. The interference probe, which has primarily been used in isothermal flows, is, however, first described in greater detail.

4.1. Interference Probes in Isothermal Flows

Interference probes are thermal-anemometry-based probes composed of two (hot-wire and/or hot-film) sensors placed close enough together that their thermal fields interfere. The interference probe used herein consists of a $10 \,\mu\mathrm{m}$ diameter tungsten wire (OH_{up} = 1.8) placed $10 \,\mu\mathrm{m}$ upstream of a $5 \,\mu\mathrm{m}$ diameter tungsten wire (OH_{down} = 1.2). In this configuration, the behavior of the downstream wire is strongly influenced by the thermal field of the upstream wire, but the latter is relatively unaffected by the presence of the former. Accordingly, the probe responds differently to changes in velocity and helium concentration, as shown in figure 4, such that simultaneous measurements of both quantities are possible. As discussed in Hewes [42] and Hewes and Mydlarski [32], the helium concentration (C) can be calculated using both output voltages of the CTA operating the two wires of the interference probe (E_{up} , E_{down}):

$$C = c_1(\ln E_{up}^2)^3 + c_2(\ln E_{down}^2)^3 + c_3(\ln E_{up}^2)^2 \ln E_{down}^2 + c_4 \ln E_{up}^2 (\ln E_{down}^2)^2 + c_5 \ln E_{up}^2 \ln E_{down}^2 + c_6 (\ln E_{up}^2)^2 + c_7 (\ln E_{down}^2)^2 \ln + c_8 \ln E_{up}^2 + c_9 \ln E_{down}^2 + c_{10}.$$
(6)

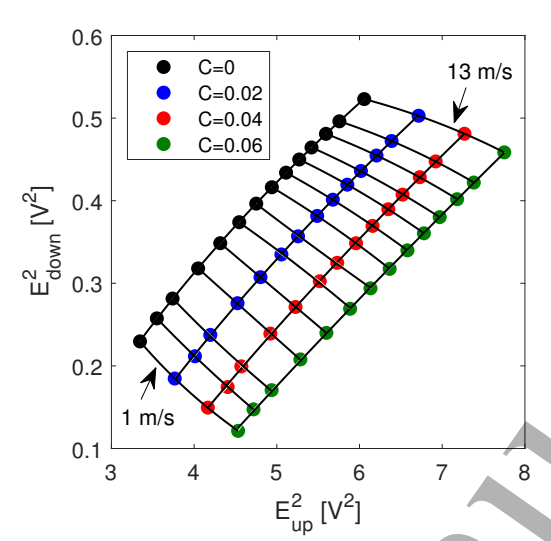


Figure 4: Calibration map for the interference probe in isothermal flow. The squared voltage of the downstream wire is plotted as a function of the squared voltage of the upstream wire for velocities ranging from 1 to 13 m/s and concentrations of 0, 0.02, 0.04, and 0.06 He mass fraction. Power laws are fit to the data along iso-concentration and iso-velocity lines.

The velocity (U) can then be obtained by applying King's Law to the upstream wire of the probe:

$$U = \left[\frac{E_{up}^2 - A(C)}{B(C)}\right]^{1/n_{up}}.$$
(7)

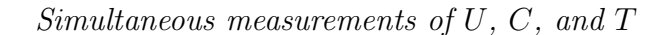
Additional information on the underlying theory, design, operation, and validation of the interference probe is provided in the aforementioned works.

4.2. Description of the Temperature Compensation Method

As previously stated, Sirivat and Warhat [1] operated an interference probe in non-isothermal flows by assuming that it was insensitive to (very) small variations in the fluid temperature. However, in many cases, including the present work, where temperature differences are on the order of 10°C, such an assumption is not possible. As may be observed in figure 5, the interference probe used herein is indeed sensitive to changes to the ambient temperature (similar to a hot-wire anemometry sensor), and a temperature compensation method is therefore required.

The temperature compensation method developed herein involves first compensating for the effects of fluid temperature changes on the upstream wire of the interference probe, and then compensating for their effects on the downstream wire. The former can be done using compensation techniques developed for single-normal hot-wire probes (e.g. Ch. 7 of [4] or [44–46]). To this end, the interference probe was calibrated over a range of velocities in flows of different fixed temperatures and concentrations. (See figure 5.) King's Law:

$$E_{up}^{2} = A(C,T) + B(C,T)U^{n_{up}},$$
(8)



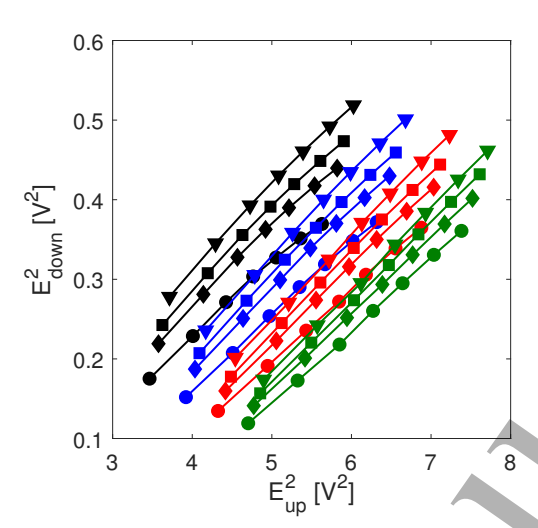


Figure 5: Calibration map for the interference probe in flows of different temperatures. The squared voltage of the downstream wire is plotted as a function of the squared voltage of the upstream wire for (i) velocities ranging from 1 to 13 m/s, (ii) concentrations of 0 (black), 0.02 (blue), 0.04 (red), and 0.06 (green) He mass fraction, and (iii) temperatures of nominally 303K (\Box) 293K (\bigtriangledown) , 298K (\diamondsuit) , and 308K (\bigcirc) .

is then fit to data from the upstream wire of the probe using a constant value of n_{up} (obtained by calculation of its average value for all calibrations of different temperatures and concentrations). As may be observed in figure 6, the coefficients A and B from these calibrations are (approximately) linear functions of the flow temperature (T). Accordingly, they can be expressed as:

$$A = A^*(C)[T_{w,A} - T], \text{ and}$$
 (9)

$$B = B^*(C)[T_{w,B} - T], \tag{10}$$

and the effective average temperature of the upstream wire $(T_{w,up})$ can be defined as:

$$T_{w,up} = \frac{1}{2}(T_{w,A} + T_{w,B}). \tag{11}$$

As demonstrated in figure 7, $T_{w,up}$ can be used to compensate for the effects of temperature on the upstream wire, since the non-isothermal data of figure 5 collapse very well when E_{up} is normalized by the temperature difference $T_{w,up}-T$. (Note that for the range of temperatures employed in the present work, the above method is sufficient, and there is no need to account for changes in the thermophysical properties of the fluid, which are assumed to be negligibly small.)

Compensating for the effects of temperature on the downstream wire is more complex, since the behavior of that wire is strongly influenced by the thermal wake of upstream wire, and King's Law may therefore not apply. As observed in figure 4, when E_{down}^2 is plotted as a function of E_{up}^2 , the iso-concentration curves exhibit power-law behaviors. Given that (i) this power-law behavior is also observed in the non-isothermal calibration map (figure 5), and (ii) it is beneficial to separate temperature-dependent



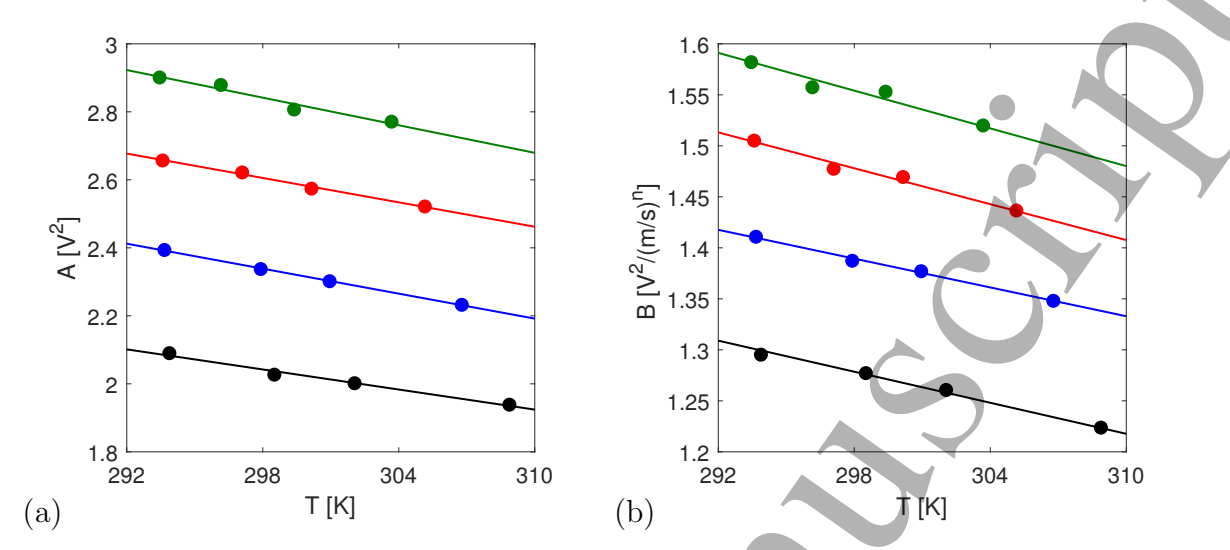


Figure 6: (a) Temperature dependence of A fit with equation (9). (b) Temperature dependence of B fit with equation (10). The concentrations of helium correspond to: C = 0: (\bullet); C = 0.02 (\bullet); C = 0.04 (\bullet); and C = 0.06 (\bullet).

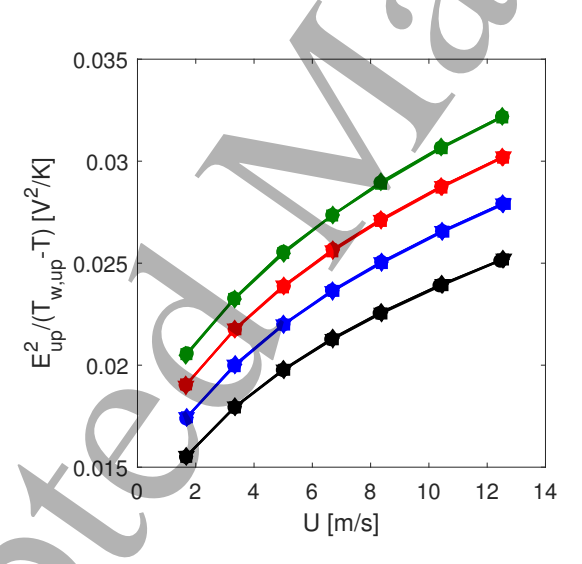


Figure 7: Temperature compensation of the upstream wire of the interference probe. Compensated voltages of the upstream wire $(E_{up}/(T_{w,up}-T))$ are plotted as a function of U for (i) velocities ranging from 1 to 13 m/s, (ii) concentrations of 0 (black), 0.02 (blue), 0.04 (red), and 0.06 (green) He mass fraction, and (iii) temperatures of nominally 303K (\Box) 293K (\Diamond), and 308K (\bigcirc).

terms from temperature-independent terms (denoted by *), we propose the following expression to the relate the voltage of the downstream wire of the interference probe to that of the upstream wire:

$$E_{down}^{2} = F(C,T) + G(C,T) \left[\frac{E_{up}^{2}}{T_{w,up} - T} \right]^{n_{down}}.$$
 (12)

Similar to the upstream wire, F and G are also found to be linear functions of the fluid

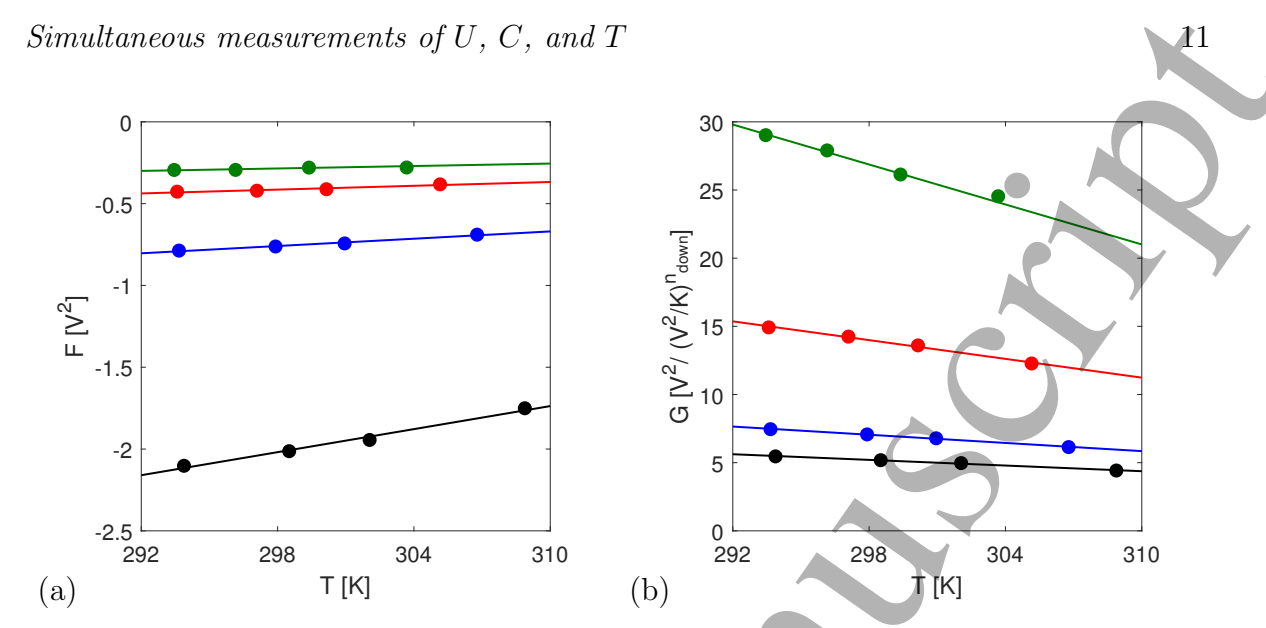


Figure 8: (a) The coefficient F plotted as a function of T and fit with equation (13). (b) The coefficient G plotted as a function of T and fit with equation (14). The concentrations of helium correspond to: C = 0: (\bullet); C = 0.02 (\bullet); C = 0.04 (\bullet); and C = 0.06 (\bullet).

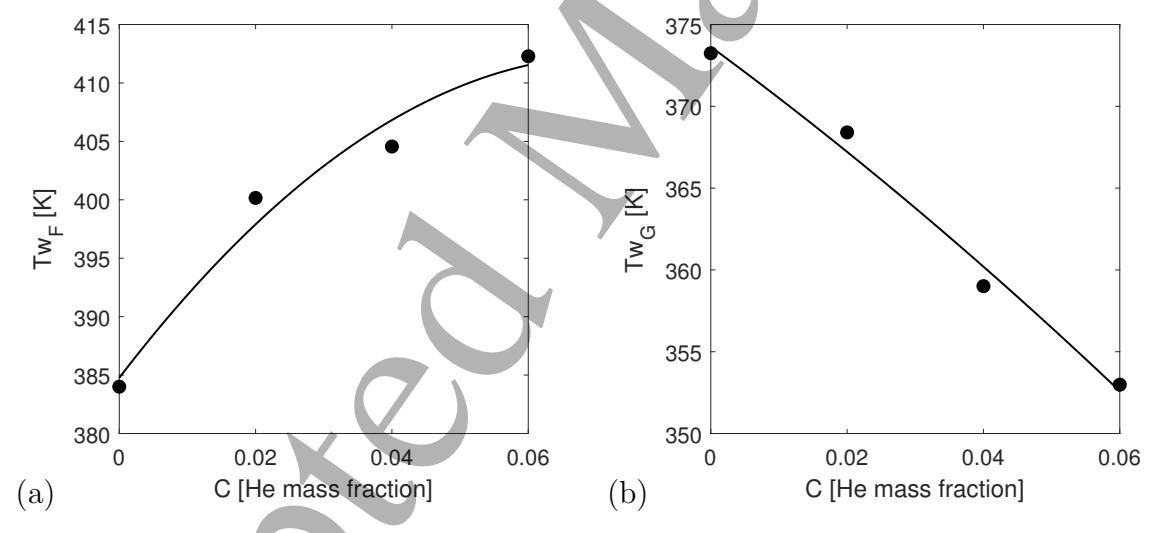


Figure 9: Dependence of (a) $T_{w,F}$ and (b) $T_{w,G}$ on helium concentration (C). Second-order polynomials are fit to the data.

temperature:

$$F = F^*(C)[T_{w,F}(C) - T], \text{ and}$$
 (13)

$$G = G^*(C)[T_{w,G}(C) - T], (14)$$

as demonstrated in figure 8. However, in contrast to the upstream wire, the calibration constants $T_{w,F}$ and $T_{w,G}$ depend on helium concentration, as may be observed in figure 9. This adds complexity to the compensation process, as compensating for the effects of temperature requires knowledge of the concentration, and solving for concentration requires compensating for temperature.

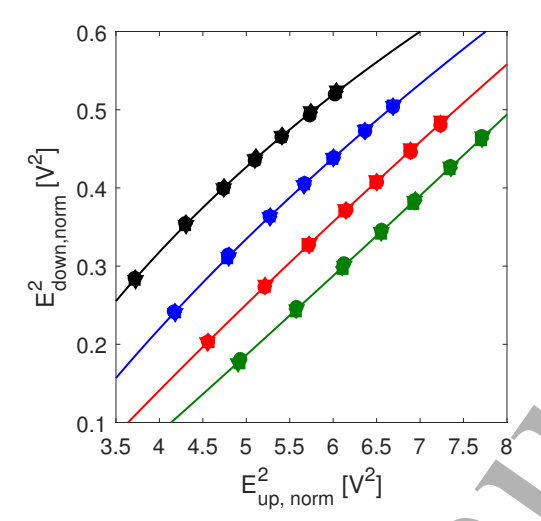


Figure 10: Temperature-normalized calibration map of the interference probe. The expected downstream wire voltage at 20°C ($E_{down,norm}$) is plotted as function of the expected upstream wire voltage at 20°C ($E_{up,norm}$) for (i) velocities ranging from 1 to 13 m/s, (ii) concentrations of 0 (black), 0.02 (blue), 0.04 (red), and 0.06 (green) He mass fraction, and (iii) temperatures of nominally 303K (\square) 293K (∇), 298K (\Diamond), and 308K (\bigcirc).

The following method to compensate for temperature is therefore suggested. The calibration data is first used to calculate the expected upstream and downstream wire voltages at 20°C (an arbitrary reference value chosen to normalize the calibration map):

$$E_{up,norm}^{2} = \frac{E_{up}^{2}}{T_{w,up} - T} (T_{w,up} - T_{20}), \tag{15}$$

$$E_{down,norm}^{2} = F^{*}(T_{w,F} - T_{20}) + G^{*}(T_{w,G} - T_{20}) \left(\frac{E_{up}^{2}}{T_{w,up} - T}\right)^{n_{down}}. \tag{16}$$

$$E_{down,norm}^2 = F^*(T_{w,F} - T_{20}) + G^*(T_{w,G} - T_{20}) \left(\frac{E_{up}^2}{T_{w,un} - T}\right)^{n_{down}}.$$
 (16)

Analysis of the calibration data, for which the concentration is known, and for which F^* , G^* , $T_{w,F}$ and $T_{w,G}$ can be calculated, shows that when $E_{down,norm}$ is plotted as as a function of $E_{up,norm}$, calibrations at different temperatures collapse exceptionally well (see figure 10) and resemble the isothermal calibration map presented in figure 4. Thus, provided the upstream and downstream wire voltages are replaced by their values normalized by a reference temperature (20°C in this case), concentration and velocity can then be calculated using equations (6) and (7). However, given that concentration is required to calculate the normalized value of the downstream wire $(E_{down,norm})$ (as well as $F, G, T_{w,F}$, and $T_{w,G}$) an iterative process must be employed to solve for the concentration.

5. Validation of the Temperature Compensation Method

The temperature compensation method proposed above was then validated by performing measurements with the 3-wire probe along the centerline of the coaxial

Table 2: Experimental properties of center jet, annular jet, and coflow for validation measurements. Note that H and nH are respectively used to refer to cases with and without helium, and that T and nT are respectively used to refer to cases with and without the heated coflow.

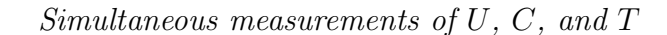
Case	C_1	$T_3 - T_1$ (K)	$Re_{D_h,1}$	$Re_{D_h,2}$	$ ho_1/ ho_2$	$ ho_1/ ho_3$	$U_3 \text{ (m/s)}$
I: H & T	0.04	5.95	3900	2300	0.8	0.8	0.4
II: nH & T	0	5.95	4500	2300	1.0	1.0	0.4
III: H & nT	0.04	-1.10	3900	2300	0.8	0.8	0.4
IV: nH & nT	0	-1.10	4500	2300	1.0	1.0	0.4

jet apparatus described in §2.2. As stated earlier, the 3-wire probe is composed of an interference probe and cold-wire thermometer. Both probes are placed approximately 1 mm apart, and operated simultaneously, such that three output voltages are acquired. Since the cold-wire has been shown to be insensitive to velocity and helium concentration, temperature can be measured independently of both these quantities. Thus, measurements from the cold-wire can be used to compensate for the effects of temperature on the interference probe.

The validation measurements were performed in four different flows, the properties of which are summarized in table 2. In cases I and III, a He/air mixture ($C_1 = 0.04$) was supplied to the center jet, whereas in cases II and IV, pure air was supplied to the center jet. All four cases were used in the validation measurements, but cases II and IV had an additional purpose, as they were used to quantify any noise in the concentration measurements (see Hewes and Mydlarski [32]). During post-processing, all four sets of data were Fourier transformed to obtain spectra, and a Wiener filter was applied to the data. After accounting for noise in the concentration measurements, the velocity field was re-calculated. Furthermore, to improve the accuracy of the concentration measurements, mean concentrations measured in flows of pure air were subtracted from the concentration measurements in He/air mixtures.

To demonstrate the effectiveness of the temperature compensation method, measurements in turbulent flows with different temperature fields, but identical velocity and concentration fields, were compared. In cases I and II, the coflow was heated such that it was 5.95°C hotter than the center jet, whereas in cases III and IV the coflow was not heated. (In these cases the temperature of the coflow was slightly lower than that of the center jet due to the Joule-Thompson effect.) Although the temperature fields of cases III and IV were distinct from those of cases I and II, the maximum temperature temperature differences in all flows were less than 6°C. Thus, temperature could be considered a passive scalar, which should have no effect on either the velocity or concentration fields of the flow.

Figures 11 and 12 depict the velocity and concentration fields measured by the 3-wire probe along the axis of the coaxial jets. Although some differences can be observed between flows which contain helium (I & III) and those which do not (II & IV) (due to



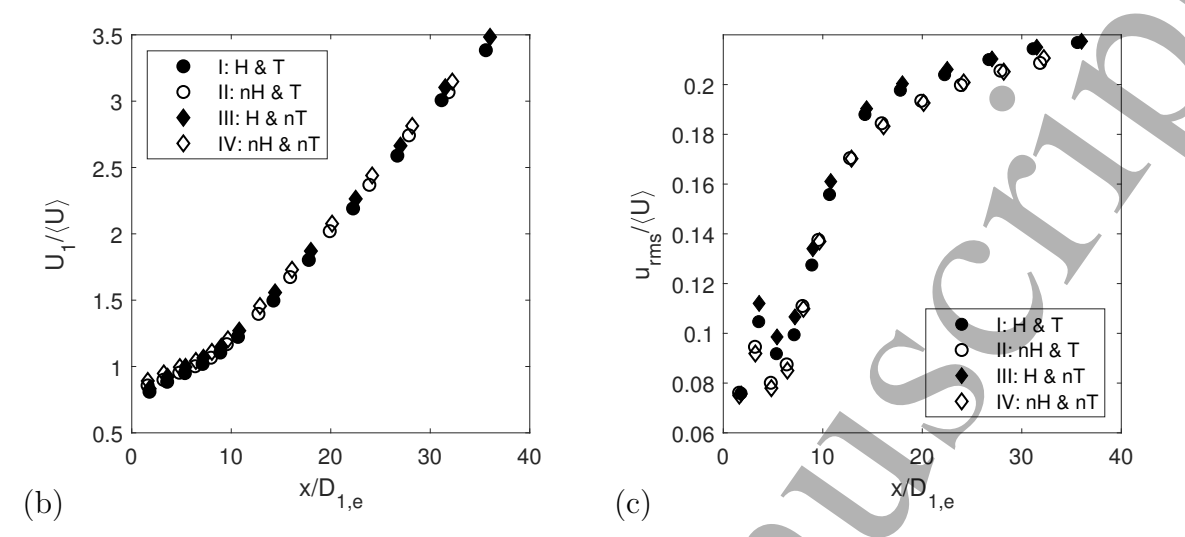


Figure 11: Downstream evolution of (a) $U_1/\langle U \rangle$, and (b) $u_{rms}/\langle U \rangle$ along the centerline of the coaxial jets for the four validation test cases presented in table 2. Measurements are normalized by the effective diameter of the center jet $(D_{1,e} = \sqrt{\rho_1/\rho_3}D_1)$ to account for density differences [42] (see also [47,48]).

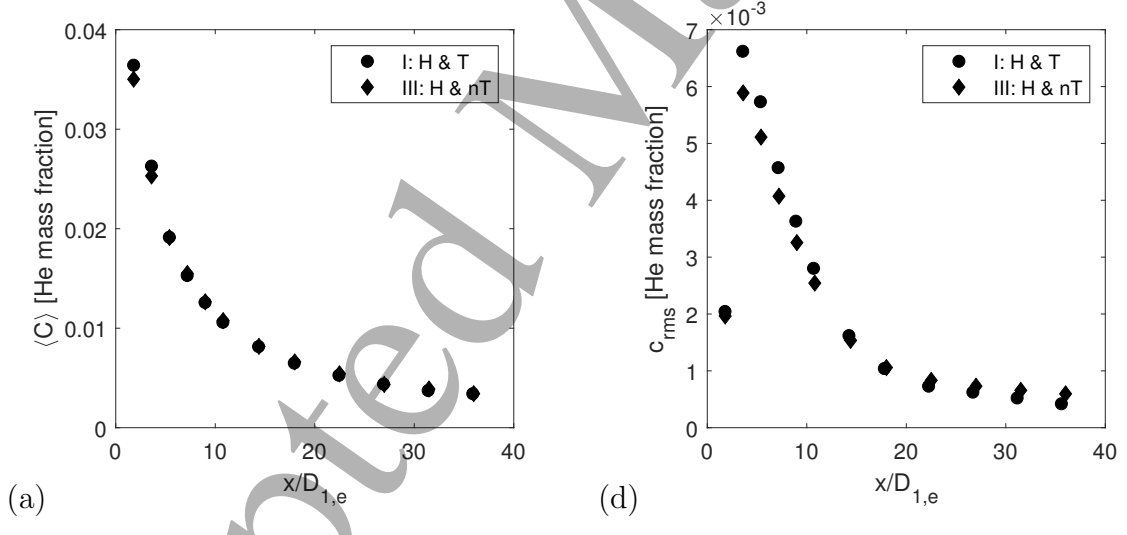


Figure 12: Evolution of (a) $\langle C \rangle$, and (b) c_{rms} along the centerline of the coaxial jets for the two validation test cases presented in table 2 in which a He/air mixture ($C_1 = 0.04$) was supplied to the center jet. Measurements are normalized by the effective diameter of the center jet ($D_{1,e} = \sqrt{\rho_1/\rho_3}D_1$) to account for density differences [42] (see also [47,48]).

the effects of variable density in cases I & III [42]), as expected, measurements from cases in which the coflow was heated (I & II) collapse onto the equivalent cases in which the coflow was not heated (III & IV). Accordingly, it can be concluded that the temperature compensation described in the previous subsection correctly accounts for the effects of temperature on the interference probe.

Using the temperature compensation method, the 3-wire probe can measure velocity and concentration in turbulent flows containing helium and temperature fluctuations

Simultaneous measurements of U, C, and T

with uncertainties of 0.20 m/s and 0.0002 He mass fraction, respectively. These values are comparable to those for an interference probe in isothermal flows. Moreover, the uncertainty for the velocity is approximately equal to that calculated for a single-normal hot-wire in an isothermal flow of pure air [42].

6. Conclusions

In the present work, we have (i) demonstrated that a cold-wire thermometer is effectively insensitive to the helium concentration, and (ii) developed and (iii) validated a novel temperature compensation technique for interference probes, thus extending their use to non-isothermal flows. Moreover, when the cold-wire thermometer and interference probe are placed side-by-side to form a 3-wire thermal-anemometry-based probe, it is possible to simultaneously measure velocity, helium concentration, and temperature in turbulent flows. In contrast to a previous thermal-anemometry-based probe developed by Sirivat and Warhat [1], the 3-wire probe developed herein can be employed to obtain multi-scalar and velocity statistics in flows with substantial temperature variations. Given the paucity of such measurements in the literature, use of such probes to simultaneously measure velocity, concentration, and temperature is expected to enhance our understanding of multi-scalar mixing, including applications of differential diffusion.

Acknowledgments

This work was graciously funded by the Natural Sciences and Engineering Research Council (NSERC) of Canada (grant number RGPIN-2018-05848).

Appendix A. Nomenclature

```
A, B numerical constants
```

C concentration (He mass fraction)

 C_1 concentration at exit of center jet

 c_i numerical constants

 c_w specific heat of wire material

 D_e effective diameter

 D_h hydraulic diameter

d diameter of wire

E wire voltage

F, G numerical constants

I wire current

k thermal conductivity of fluid

l length of wire

n numerical constant (exponent in King's Law)

Nu Nusselt number

OH overheat ratio ($\equiv R_w/R_a$) of wire

 R_{20} resistance of wire at 20°C

 R_a cold-resistance of wire

- R_w resistance of wire (while being operated)
- Re Reynolds number
- T temperature of the fluid
- T_w temperature of wire
- U velocity of the fluid
- U_1 average velocity at exit of center jet
- x cylindrical coordinate
- α_{20} temperature coefficient of resistivity of wire material at 20°C
- θ temperature difference
- ρ density of fluid
- ρ_w density of wire material

Additional subscripts and superscripts

- * independent of temperature
- 1 center jet
- 2 annular jet
- 3 coflow
- A with respect to constant A
- B with respect to constant B
- down downstream wire
- F with respect to constant F G with respect to constant G
- rms root mean square up upstream wire

Operators

⟨ ⟩ mean value

References

- [1] Sirivat A and Warhaft Z 1982 J. Fluid Mech. 120 475
- [2] Perry A 1982 Hot-wire anemometry (Clarendon Press)
- [3] Lomas C 1986 Fundamentals of hot wire anemometry. (Cambridge University Press)
- [4] Bruun H 1995 Hot-wire Anemometry: Principles and Signal Analysis (Oxford University Press)
- [5] Tropea C, Yarin A and Foss J 2007 Springer Handbook of Experimental Fluid Mechanics (Springer)
- [6] Lemay J and Benaïssa A 2001 Exp. Fluids **31** 347–356
- [7] Lepore J and Mydlarski L 2011 J. Fluid Mech. 678 417–450
- [8] Arwatz G, Bahri C, Smits A J and Hultmark M 2013 Meas. Sci. Technol. 24 125301
- [9] Ng W F and Epstein A H 1983 Rev. Sci. Instrum. 54 1678–1683
- [10] Ahmed S and So R 1986 Exp. Fluids 4 107–113
- [11] Birch A D, Brown D R, Dodson M G and Swaffield F 1986 J. Phys. E: Sci. Instrum. 19 59-63
- [12] White B 1987 Bound.-Lay. Meteorol. 38 105–124
- [13] Ninnemann T and Ng W 1992 Exp. Fluids 13 98–104
- [14] Guibert P and Dicocco E 2002 Exp. Fluids 32 494–505
- [15] Cabannes M, Ferchichi M and Tavoularis S 2004 Meas. Sci. Technol. 15 1211
- [16] Wyngaard J and Coté O 1971 J. Atmos. Sci. 28 190–201
- [17] Venkataramani K, Tutu N and Chevray R 1975 Phys. Fluids 18 1413–1420
- [18] Ferchichi M and Tavoularis S 2002 J. Fluid Mech. **461** 155–182
- [19] Mydlarski L 2003 J. Fluid Mech. 475 173–203

- [20] Beaulac S and Mydlarski L 2004 Phys. Fluids 16 3161–3172
- [21] Berajeklian A and Mydlarski L 2011 Phys. Fluids 23 055107
- [22] Lepore J and Mydlarski L 2012 J. Fluid Mech. 713 453–481
- [23] Way J and Libby P 1970 AIAA J. 8 976–978
- [24] Way J and Libby P 1971 AIAA J. 9 1567–1573
- [25] McQuaid J and Wright W 1973 Intl. J. Heat Mass Transfer 16 819–828
- [26] McQuaid J and Wright W 1974 Intl. J. Heat Mass Transfer 17 341–349
- [27] Stanford R A and Libby P 1974 Phys. Fluids 17 1353
- [28] Panchapakesan N and Lumley J 1993 J. Fluid Mech. 246 225
- [29] Harion J L, Favre-Marinet M and Camano B 1996 Exp. Fluids 22 174–182
- [30] Sakai Y, Watanabe T, Kamohara S, Kushida T and Nakamura I 2001 Int. J. Heat Fluid Fl. 22 227–236
- [31] Lehavi A, Yona D, Costandi G, Weissman A and Katz Y 2015 Glob. Anaesth. Perioper. Med. 1 104–106
- [32] Hewes A and Mydlarski L 2021 Meas. Sci. Technol. 32 105305
- [33] Warhaft Z 1984 J. Fluid Mech. 144 363
- [34] Tong C and Warhaft Z 1995 J. Fluid Mech. 292 1–38
- [35] Saylor J and Sreenivasan K 1998 Phys. Fluids 10 1135–1146
- [36] Costa-Patry E and Mydlarski L 2008 J. Fluid Mech. 609 349–375
- [37] Lavertu T, Mydlarski L and Gaskin S 2008 J. Fluid Mech. 612 439-475
- [38] Cai J, Dinger M, Li W, Carter C, Ryan M and Tong C 2011 J. Fluid Mech. 685 495–531
- [39] Soltys M and Crimaldi J 2015 J. Fluid Mech. 769 130–153
- [40] Li W, Yuan M, Carter C and Tong C 2017 J. Fluid Mech. 817 183–216
- [41] Shoaei F and Crimaldi J 2017 Exp. Fluids 58 26
- [42] Hewes A 2020 Multi-Scalar Mixing in Turbulent Coaxial Jets Ph.D. thesis McGill University
- [43] Lepore J Experiments on passive scalar mixing in turbulent flows with different velocity and scalar-field boundary conditions Ph.D. thesis McGill University
- [44] Bremhorst K 1985 J. Phys. E: Sci. Instrum. 18 44-49
- [45] Lienhard J H and Helland K N 1989 Exp. Fluids 7(4) 265–270
- [46] Hultmark M and Smits A 2010 Meas. Sci. Technol. 21 105404
- [47] Dowling D R and Dimotakis P E 1990 J. Fluid Mech. 218 109–141
- [48] Mi J, Nobes D and Nathan G 2001 J. Fluid Mech. 432 91–125